Available online at www.sciencedirect.com
SCIENCE DIRECT
Dyes and Pigments 71 (2006) 153–160
DYES and PIGMENTS
www.elsevier.com/locate/dyepig

The synthesis and properties of unsymmetrical 3,7-diaminophenothiazin-5-ium iodide salts: Potential photosensitisers for photodynamic therapy

Stephen A. Gorman [a,*], Andrea L. Bell [b], John Griffiths [a], Dave Roberts [b], Stanley B. Brown [c]

[a] *Department of Colour and Polymer Chemistry, Centre for Photobiology and Photodynamic Therapy, The University of Leeds, Leeds LS2 9JT, UK*
[b] *School of Biomedical Sciences, Centre for Photobiology and Photodynamic Therapy, University of Leeds, Leeds LS2 9JT, UK*
[c] *School of Biochemistry and Microbiology, Centre for Photobiology and Photodynamic Therapy, University of Leeds, Leeds LS2 9JT, UK*

Received 6 June 2005; accepted 23 June 2005
Available online 19 August 2005

Abstract

A series of unsymmetrical 3,7-(*N*,*N*-disubstituted-amino)-phenothiazin-5-ium iodides have been prepared by stepwise reaction of secondary amines with phenothiazin-5-ium tetraiodide hydrate. The singlet oxygen generating efficiencies and polarity characteristics of the dyes are compared with those of Methylene Blue, and the factors influencing the potential value of these compounds as photosensitisers for photodynamic therapy are discussed. Preliminary data for the in vivo anti-tumour efficacy of the compounds suggest that high lipophilicity is an important requirement for high activity.

Keywords: Photodynamic therapy; Phenothiazinium sensitisers; In vivo anti-tumour efficacy

1. Introduction

Photodynamic therapy (PDT) involves administration of a photosensitiser (or a metabolic precursor of the photosensitiser in the case of aminolevulinic acid treatment) to the patient, followed by activation of the photosensitiser by light once it has localised preferentially in the tumour tissue. Destruction of the diseased cells is thus brought about in a highly targeted manner. It is generally accepted that the dominant mechanism leading to cell destruction is a Type II (singlet oxygen mediated) process, and consequently good PDT photosensitisers must be efficient singlet oxygen sensitisers. In addition, they must have low general toxicity, and should show some degree of selectivity for malignant tissue over normal tissue. For maximum efficacy, the photosensitiser should also be capable of excitation by light of relatively long wavelengths (>ca. 600 nm, the 'therapeutic window') in order to maximise penetration of the light through tissue. Currently, much research effort is being directed towards the development of improved photosensitisers, the prime objectives being to achieve greater tumour selectivity, increased singlet oxygen generating efficiency, and decreased skin photosensitisation.

The potential of PDT for the treatment of many types of disease was recognised more than 25 years ago, yet it is only relatively recently that PDT has started to gain acceptance in the clinic. In recent years, PDT photosensitisers and their metabolic precursors have been

* Corresponding author. Tel.: +44 113 343 2930; fax: +44 113 343 2947.
E-mail address: ccdsag@leeds.ac.uk (S.A. Gorman).

0143-7208/$ - see front matter © 2005 Elsevier Ltd. All rights reserved.
doi:10.1016/j.dyepig.2005.06.011

investigated for many types of cancers [1–3] and pre-cancerous conditions, e.g. Barrett's oesophagus [4,5]. PDT has also been investigated for the palliation of several types of advanced cancers [6–11], and for the treatment of certain non-malignant conditions, such as psoriasis [12], age-related macular degeneration [13] and microbial infections [14,15].

At present there are four photosensitising drugs clinically approved for the PDT of cancer [1]: *Porfimer sodium*, the generic name for haematoporphyrin derivative; *Temoporfin*, the generic name for methyl-tetrahydroxyphenyl chlorin; and two metabolic precursor drugs based on the aminolevulinic moiety. All these drugs suffer from certain specific drawbacks, namely prolonged skin photosensitisation following administration, and poor light absorption above 600 nm (thus limiting the treatment of deep tumours). Another drawback specific to Porfimer sodium is chemical heterogeneity. We have therefore investigated the suitability of certain cationic phenothiazinium dyes as alternative PDT sensitisers, as these do not suffer from any of these disadvantages.

The 3,7-diaminophenothiazin-5-ium cations in general exhibit an intense absorption band (ε ca. 100,000 $dm^3\,mol^{-1}\,cm^{-1}$) in the 600–660 nm region, appropriate to the 'therapeutic window' for PDT, allowing efficient tissue penetration by the irradiating light. They also compare favourably with porphyrins and phthalocyanines with respect to their ability to generate singlet molecular oxygen, $O_2(^1\Delta_g)$. Methylene Blue has long been used as a standard for singlet molecular oxygen rate determination experiments, and has a quantum yield for the formation of $O_2(^1\Delta_g)$ of $\phi_\Delta = 0.50$ in methanol, which is virtually unchanged in water [16]. This can be contrasted with hematoporphyrin, with a value of $\phi_\Delta = 0.74$ in methanol which decreases to 0.42 in water [16,17]. This decrease in quantum yield is attributed to aggregation in aqueous media [17], and is a general feature of most porphyrins and phthalocyanines, with obvious implications for their application as PDT photosensitisers. The phenothiazinium dyes are also readily synthetically available in pure form, and do not form isomeric mixtures.

The best-known example of this class is Methylene Blue (MB) (Fig. 1, **1**). MB was originally developed as a textile dye, and its first biological use was as a vital stain [18]. Interestingly, it was used in the treatment of inoperable human cancers at the turn of the 20th century [19] though not as part of a concerted PDT regimen. Since then, MB and a very small number of its derivatives have also been investigated for applications in the PDT treatment of superficial bladder cancer [20,21], as photoactivated antimicrobial agents [22,23] and more recently as a photoactivated viral disinfectant for blood [24,25]. It is well established that MB induces a phototoxic effect in vitro but the clinical application of this effect has been limited by a number of associated problems. Thus it shows a low or zero PDT effect in vivo following intravesical or intravenous administration, which has been attributed to the hydrophilic nature of the dye limiting tumour localisation. Consequently there is only a small difference between its light and dark toxicities. In addition, a redistribution of the dye from the lysosomes to the nucleus following illumination raises concerns regarding possible mutagenicity. Several authors have investigated the photobiological properties of other phenothiazinium compounds [26–30]. Cincotta et al. have conducted extensive studies on benzophenothiazinium photosensitisers and their phototherapeutic properties [31,32]. Wagner et al. have investigated photoinactivation of viruses using MB and a series of unsymmetrical analogues [25,33]. In all the cases, the range of structures investigated has been very small, often restricted to commercially available materials of the old textile dye type.

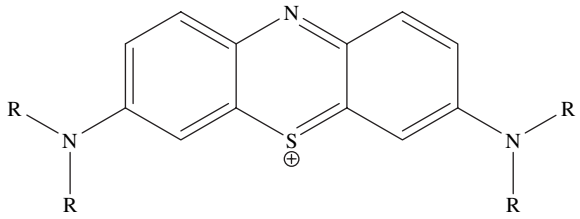

1: R = methyl
2: R = C_2-C_6 alkyl

Fig. 1. A general structure for symmetrical phenothiazinium dyes.

The present paper reports our continuing research into novel photosensitisers based on the phenothiazinium system. Earlier work has already shown that small changes to the structure of the phenothiazinium chromophore could have a marked effect on anti-microbial photoactivity [21,22] and anti-cancer photoactivity [34]. Recently we investigated structure–PDT activity relationships for a series of symmetrical phenothiazinium analogues (Fig. 1, **2**) and found that their in vitro activities towards murine fibrosarcoma (RIF-1) cells were critically dependent on alkyl chain length [35]. As an extension of that work, the corresponding in vitro PDT activities of a range of unsymmetrical phenothiazinium analogues, **3a–l**, have been measured and reported [36]. We now describe the synthesis and characterisation of the photosensitisers, **3a–l**, and report their physical properties, including a preliminary study of their in vivo PDT activity in a subcutaneously transplanted CaNT tumour mouse model.

2. Results and discussion

2.1. Synthesis

Fig. 2 illustrates the structures of the unsymmetrical phenothiazinium photosensitisers under investigation.

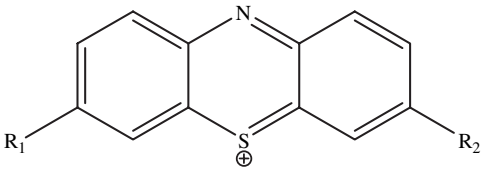

3

	R_1	R_2
a:	morpholino	$N(n\text{-Pr})_2$
b:	morpholino	$N(n\text{-Bu})_2$
c:	morpholino	$N(n\text{-C}_5\text{H}_{11})_2$
d:	diethanolamino	$N(n\text{-Pr})_2$
e:	diethanolamino	$N(n\text{-Bu})_2$
f:	diethanolamino	$N(n\text{-C}_5\text{H}_{11})_2$
g:	$N(n\text{-Pr})_2$	NMe_2
h:	$N(n\text{-Pr})_2$	NEt_2
i:	$N(n\text{-Pr})_2$	$N(n\text{-Pr})_2$
j:	$N(n\text{-Pr})_2$	$N(n\text{-Bu})_2$
k:	$N(n\text{-Pr})_2$	$N(n\text{-C}_5\text{H}_{11})_2$
l:	$N(n\text{-Pr})_2$	$N(n\text{-C}_6\text{H}_{13})_2$

Fig. 2. The unsymmetrical phenothiazinium dyes under investigation.

They differ from **1** and **2** in that they exhibit varying degrees of polar and spatial asymmetry. Three distinct series of structures with different hydrophobic/hydrophilic characteristics can be recognised. Thus **3a–c** have a polar, aprotic morpholino group on one side of the molecule, and an increasingly hydrophobic dialkylamino group on the other, the alkyl chains ranging in size from *n*-propyl to *n*-pentyl. Dyes **3d–f** have a similar range of dialkylamino groups on one side of the molecule, with a common polar, protic diethanolamino group on the other. Dyes **3g–l** contain only hydrophobic dialkylamino substituents, and have a common dipropylamino group on one side of the molecule, and a dialkylamino group on the other side, the alkyl groups ranging in size from methyl to *n*-hexyl. With such a wide range of polarity characteristics and overall molecular sizes, it was expected that these would help provide useful structure–activity relationships for designing optimised PDT photosensitisers.

Although there are several routes available for the preparation of simple phenothiazinium dyes, few are suitable for the preparation of unsymmetrical compounds as they give mixed products; the phenothiazinium dyes are notoriously difficult to separate and purify. It was decided therefore to use the synthetic route developed by Strekowski et al. [37], which allows stepwise addition of two different amino groups to the phenothiazinium nucleus. The reaction involves initial oxidation of phenothiazine with iodine to give phenothiazin-5-ium tetraiodide hydrate, which is isolated before further use. Precise, controlled addition of two molar equivalents of the first secondary amine gives the mono-substituted salt, which can be isolated and recrystallised before continuing with the second stage of the procedure. Addition of two molar equivalents of the second amine to this intermediate then gives the requisite 3,7-disubstituted phenothiazin-5-ium iodide. In the original paper by Strekowski et al., the unsymmetrical 3,7-disubstituted derivatives prepared were precipitated from the reaction solvent (methanol) in a reasonable state of purity, and required only one recrystallisation to give microanalytically pure products. However, for the analogues (**3a–l**), we found that invariably a more involved purification was required. Typically, this involved precipitation from a suitable two solvent system followed by recrystallisation until a product of constant molar absorptivity was obtained. Capillary electrophoresis was used to confirm purity. The purified dyes were characterised by electrospray mass spectrometry.

2.2. Singlet oxygen generating efficiency and partition coefficients

The photosensitisers, **3a–l**, dissolve in methanol to give blue solutions with λ_{max} values in the range 660–665 nm (Table 1). Molar absorption coefficients for this type of dye are of the order of 10^4 dm^3 mol^{-1} cm^{-1} when completely deaggregated in solution, aggregation causes lower values.

The singlet oxygen [$O_2(^1\Delta_g)$] generating efficiencies of the dyes **1** and **3a–l** are summarised in Table 1. The quantum yield for singlet oxygen generation by a dye is dependent on the rate of intersystem crossing from its S_1 excited state to the T_1 state, and also on the lifetime of the T_1 state, and efficient formation of a long-lived triplet state is essential for efficient production of singlet oxygen by energy transfer. Competing processes include

Table 1
Relative singlet oxygen generating efficiencies, λ_{max} and log *P* values for 3,7-diaminophenothiazin-5-ium dyes (**1**) and (**3a–l**)

	R_1	R_2	Relative $^1O_2$ generating efficiency[a]	λ_{max} (methanol) (nm)	Log *P*[b]
1	NMe_2	NMe_2	1.0	665	−0.9
3a	Morpholino	$N(n\text{-Pr})_2$	0.5	663	0.5
3b	Morpholino	$N(n\text{-Bu})_2$	0.5	661	1.0
3c	Morpholino	$N(n\text{-C}_5\text{H}_{11})_2$	0.4	663	1.1
3d	Ethanolamino	$N(n\text{-Pr})_2$	0.4	663	−0.1
3e	Ethanolamino	$N(n\text{-Bu})_2$	0.6	660	1.3
3f	Ethanolamino	$N(n\text{-C}_5\text{H}_{11})_2$	0.6	663	1.1
3g	$N(n\text{-Pr})_2$	NMe_2	0.8	661	−0.7
3h	$N(n\text{-Pr})_2$	NEt_2	0.9	661	1.0
3i	$N(n\text{-Pr})_2$	$N(n\text{-Pr})_2$	0.9[c]	661	1.2[c]
3j	$N(n\text{-Pr})_2$	$N(n\text{-Bu})_2$	0.9	660	1.7
3k	$N(n\text{-Pr})_2$	$N(n\text{-C}_5\text{H}_{11})_2$	0.7	663	2.0
3l	$N(n\text{-Pr})_2$	$N(n\text{-C}_6\text{H}_{13})_2$	0.9	662	>2

[a] Measured in 90% dimethyl formamide/10% water, using 1,3-diphenylisobenzofuran as singlet oxygen detector.
[b] In *n*-octanol/water.
[c] Reported in Ref. [36].

fluorescence and internal conversion. One of the reasons for the effectiveness of the MB system is the presence of sulphur in the chromophore, as the heavy atom effect of sulphur increases the rate of the $S_1 \rightarrow T_1$ intersystem crossing process relative to these competing pathways. As the dyes **1**, **2** and **3a–l** have the same underlying chromophore, one might expect them to have similar singlet oxygen generating efficiencies. In fact the values for **3a–l** range from 40 to 90% relative to MB itself. These efficiencies are comparable to those of the symmetrical dialkylamino derivatives **2** reported previously [35]. Although the experimental errors in determining the values shown in Table 1 are relatively high, nevertheless certain definite trends can be discerned. Thus the more amphiphilic dyes **3a–f**, i.e. those with morpholino or ethanolamino substituents on one side of the molecule, have singlet oxygen efficiency values in the range 40–60%, which are significantly lower than those of the more generally hydrophobic dyes **3g–l** (70–90%). This may be related to a greater tendency of the former to take part in hydrogen bonding with the water in the solvent system used; a process that could lead to a reduction in the triplet state lifetime.

Despite the range of efficiencies found for **3a–l**, all should be perfectly adequate singlet oxygen photosensitisers for PDT purposes, and any failings that individual dyes might have as PDT photosensitisers are more likely to be due to other causes, such as poor cell uptake, inappropriate cellular localisation sites, or aggregation within cells.

One factor that has an important influence on the ability of dyes to be taken up by cells is the overall hydrophilic/hydrophobic character of the molecule. This may be quantified in a relative manner by measuring the partition coefficient (P) in a suitable water/immiscible non-polar solvent system. We have shown previously [35,36] that $\log P$ values of phenothiazinium photosensitisers are important in determining the site of subcellular localisation, and thus the site of photo-oxidative damage. Phenothiazinium sensitisers were shown by fluorescence microscopy to localise initially in the lysosomes of RIF-1 murine fibrosarcoma cells, and following illumination there was a relocalisation to other sites in the cell, which could be broadly correlated to the $\log P$ value of the photosensitiser. The specific target following relocalisation throughout the cytoplasm will be greatly influenced by the lipophilicity of the photosensitiser (membrane surfaces) and its charge distribution (mitochondrial membranes). It has been shown that apoptosis is more rapid following photodamage resulting from mitochondrial localisation compared with lysosomal localisation [38].

The $\log P$ values for dyes **1** and **3a–l** have been determined for the water/*n*-octanol system, and are listed in Table 1. It can be seen that the dyes exhibit a wide range of hydrophobic/hydrophilic character. Interestingly, the dimethylamino group appears to exert the greatest effect on hydrophilicity, and this is most clearly demonstrated by comparing the dipropylamino series of dyes **3g**, **3a** and **3d**. In addition to the $-N(n\text{-Pr})_2$ group, these contain, respectively, a morpholino, diethanolamino and dimethylamino group. The most hydrophilic of these dyes is the dimethylamino derivative **3g**, with a $\log P$ value of -0.7, comparable to that of MB itself (-0.9). Surprisingly the diethanolamino derivative **3d** is much less water soluble, with a $\log P$ value of -0.1. However, it still has significantly higher hydrophilic character than the morpholino derivative **3a** ($\log P = 0.5$).

This difference between morpholino and diethanolamino groups becomes less well correlated with $\log P$ for higher homologues in the series, and for example the morpholino/dipentylamino and diethanolamino/dipentylamino dyes, **3c** and **3f**, respectively, have identical $\log P$ values.

The hydrophobicities of the dyes containing only dialkylamino groups show a predictable increase in $\log P$ with increasing overall alkyl chain length. Thus the most hydrophobic photosensitiser is the dipropylamino/dihexylamino derivative **3l**, with no measurable solubility in water and with a $\log P$ value greater than 2.

2.3. A preliminary investigation of the in vivo PDT activity of the photosensitisers, ***3a–l***

Previously we have reported the in vitro PDT activity of dyes **3a–l** towards murine fibrosarcoma (RIF-1) cells [36]. We now report some preliminary findings for the effectiveness of these photosensitisers in vivo, using a mouse model with subcutaneously transplanted CaNT tumour. Following optimisation of dose and the time interval between administering photosensitiser and treating the tumour with light, the levels of macroscopic tumour necrosis were compared to levels measured in control tumours and tumours treated with MB-mediated PDT. The results are summarised in Table 2.

It is clear that the in vivo PDT activity is very sensitive to structural changes in the series of photosensitisers **3a–l**, and that this has little to do with singlet oxygen generating efficiency, and more to do with the polarity of the molecule. The most striking feature of these results is the virtually zero PDT activity of the most polar photosensitisers, namely MB itself and, with the exception of **3f**, all the compounds containing morpholino and diethanolamino groups. These virtually inactive compounds have $\log P$ values ranging from -0.9 to $+1.3$, suggesting that hydrophilicity is closely associated with low PDT activity. Conversely, the efficacy of **3f** ($\log P = 1.1$) is most likely due to the high hydrophobicity of the *n*-pentyl groups, which compensate more than for the hydrophilicity of the ethanolamino groups.

Table 2
Maximum observed induced tumour necrosis at 72 h post-PDT

Photosensitiser	R_1	R_2	% Area of tumour necrosis ± sem
Control (no sensitiser)			7 ± 4
1	NMe_2	NMe_2	17 ± 9[a]
3a	Morpholino	$N(n\text{-Pr})_2$	14 ± 7[a]
3b	Morpholino	$N(n\text{-Bu})_2$	11 ± 7[a]
3c	Morpholino	$N(n\text{-}C_5H_{11})_2$	16 ± 5[a]
3d	Ethanolamino	$N(n\text{-Pr})_2$	17 ± 10[a]
3e	Ethanolamino	$N(n\text{-Bu})_2$	3 ± 2[a]
3f	Ethanolamino	$N(n\text{-}C_5H_{11})_2$	75 ± 4[b]
3g	$N(n\text{-Pr})_2$	NMe_2	34 ± 2[a]
3h	$N(n\text{-Pr})_2$	NEt_2	49 ± 11[a]
3i	$N(n\text{-Pr})_2$	$N(n\text{-Pr})_2$	56 ± 7[a]
3j	$N(n\text{-Pr})_2$	$N(n\text{-Bu})_2$	79 ± 7[b]
3k	$N(n\text{-Pr})_2$	$N(n\text{-}C_5H_{11})_2$	72 ± 9[b]
3l	$N(n\text{-Pr})_2$	$N(n\text{-}C_6H_{13})_2$	85 ± 2[b]

[a] 16.7 μmol/kg dose.
[b] 8.35 μmol/kg dose.

However, it is clearly over-simplistic to relate log *P* values directly to PDT activity, as there are several significant anomalies. For example, whereas **3f** ($\log P = 1.1$) has high activity, the morpholino analogue **3c**, with an identical log *P* value, shows little activity. Furthermore, compounds **3g** and **3h** (log *P* values −0.7 and +1.0, respectively) are significantly more hydrophilic than **3f** and yet exhibit good PDT activity, although admittedly at a somewhat lower level than observed with the more hydrophobic photosensitisers, **3j–l**. Nevertheless, it is clear that high PDT activity in this class of photosensitiser is related to high hydrophobicity.

Several other factors need to be considered when examining structure–activity relationships in a series of closely related PDT photosensitisers, such as the influence of structure on the optimum dose, the optimum drug-to-light time interval, the optimum light dose, tumour selectivity, and the persistence of highly undesirable skin photosensitisation. The results of such investigations for the series of compounds **3a–l** will be the subject of a further paper.

3. Experimental

3.1. Determination of partition coefficients

A solution of the dye (150 μL; 100 μg/mL in DMSO) was added to a mixture of 1425 μL 1-octanol-saturated 0.1 M potassium phosphate buffer (pH 7) and 1425 μL buffer-saturated 1-octanol and vortexed. Samples were centrifuged (3500 rpm × 10 min.), 1 mL removed from each phase and the dye concentration determined by measuring the absorbance at the λ_{max} compared to standards. The log partition coefficient was calculated as $\log_{10}$ (concentration in octanol/concentration in buffer).

3.2. Singlet oxygen sensitising efficiencies

A solution containing 1,3-diphenylisobenzofuran (20 mg/dm^3) and the sensitiser (100 mg/dm^3) in 90% dimethylformamide/10% water was illuminated at 0 °C with filtered light from a parallel focused 500 W quartz halogen projector lamp. The light beam was passed through three filter solutions: aqueous copper sulphate solution, aqueous Congo Red solution and a dichloromethane solution of an infrared dye with an absorption maximum at 800 nm. The concentration of each solution was adjusted to give a transmission window with approximately 30% transmittance between 600 and 700 nm and <0.5% transmittance below 600 nm and above 700 nm. The solutions were sealed under air in 1 cm pathlength cells and exposed to the light source in a rotating carousel to ensure uniform light exposure of each solution. Photo-oxidation of diphenylisobenzofuran was monitored by observing the decrease in absorbance at 410 nm. In all runs, a corresponding solution containing Methylene Blue was used as reference.

3.3. In vivo PDT assay

In a method developed in our Centre [39], PDT-induced tumour necrosis was investigated in CBA/Gy mice bearing a subcutaneous CaNT tumour. Tumours were illuminated superficially 60 J/cm^2 (50 mW/cm^2, 660 nm ± 15 nm (FWHM)) of light from a Paterson xenon arc lamp following intravenous administration of the photosensitiser. After 72 h post-illumination the percentage area of induced tumour necrosis was determined by processing images of tumour sections.

3.4. Synthesis of photosensitisers

The following compounds were obtained from commercial sources and were used without further purification: 10*H*-phenothiazine, iodine, morpholine, *N*,*N*-diethanolamine, *N*,*N*-dimethylamine hydrochloride, *N*,*N*-dipropylamine, *N*,*N*-dibutylamine, *N*,*N*-dipentylamine, *N*,*N*-dihexylamine, *N*,*N*-diethylamine, triethylamine.

3.4.1. Preparation of phenothiazin-5-ium tetraiodide hydrate

A solution of iodine (33 mmol) in chloroform (400 cm^3) was added over a period of 1.5 h to a stirred solution of phenothiazine (10 mmol) in chloroform (100 cm^3), cooled to below 5 °C in an ice bath. The mixture was stirred for 30 min and the resultant precipitate of phenothiazin-5-ium tetraiodide hydrate was collected by filtration, washed with chloroform until free of iodine and then dried at room temperature under vacuum.

*3.4.2. General procedure for synthesis of unsymmetrical phenothiazin-5-ium iodide salts **3***

A solution of the appropriate first amine (3.6 mmol) in methanol (50 cm^3) was added dropwise at room temperature to a stirred solution of phenothiazin-5-ium tetraiodide hydrate (1.4 mmol) in methanol (300 cm^3) over a period of 60 min, and the mixture was then stirred for a further 14 h. The volume of the reaction mixture was then reduced by evaporation and the hot concentrated solution left to cool. The deposited solid was collected by filtration, washed with diethyl ether and dried. To a solution of this salt (0.34 mmol) in dichloromethane (100 cm^3) was added a solution of triethylamine (0.40 mmol) in dichloromethane (5 cm^3) followed by a solution of the appropriate second amine (1.4 mmol) in dichloromethane (50 cm^3) over a period of 60 min, and the reaction mixture was stirred at room temperature for a further 14 h. The reaction mixture was then washed successively with dilute hydrochloric acid (4×25 cm^3) and water (2×25 cm^3). The organic layer was then dried over anhydrous $MgSO_4$. The majority of the solvent was removed by rotary evaporation and an excess of diethyl ether added to precipitate the solid. The solid was collected by filtration, washed with diethyl ether and dried. Further purification of the salt, if necessary, was carried out by flash column chromatography and recrystallisation from a suitable solvent. The purity of the product was confirmed by thin layer chromatography, which showed a single blue spot.

*3.4.3. 3-N,N-Dipropylamino-7-morpholinophenothiazin-5-ium iodide, **3a***

This was obtained following isolation of 3-*N*,*N*-dipropylaminophenothiazin-5-ium triiodide and subsequent treatment with morpholine. Precipitation from dichloromethane by the addition of diethyl ether yielded **3a** as purple lustrous crystals with 23% yield. Mass spectrometry (ESI): $C_{22}H_{28}N_3OS$ requires $m/z = 382$; found $m/z = 382$.

*3.4.4. 3-N,N-Dibutylamino-7-morpholinophenothiazin-5-ium iodide, **3b***

This was obtained following isolation of 3-*N*,*N*-dibutylaminophenothiazin-5-ium triiodide and subsequent treatment with morpholine. Precipitation from dichloromethane by the addition of diethyl ether yielded **3b** as purple lustrous crystals with 22% yield. Mass spectrometry (ESI): $C_{24}H_{32}N_3OS$ requires $m/z = 410$; found $m/z = 410$.

*3.4.5. 3-N,N-Dipentylamino-7-morpholinophenothiazin-5-ium iodide, **3c***

This was obtained following isolation of 3-*N*,*N*-dipentylaminophenothiazin-5-ium triiodide and subsequent treatment with morpholine. Precipitation from dichloromethane by the addition of diethyl ether yielded **3c** a purple powder (18%). Mass spectrometry (ESI): $C_{26}H_{36}N_3OS$ requires $m/z = 438$; found $m/z = 438$.

*3.4.6. 3-N,N-Diethanolamino-7-N,N-dipropylamino-phenothiazin-5-ium iodide, **3d***

This compound was obtained following isolation of 3-*N*,*N*-dipropylaminophenothiazin-5-ium triiodide and subsequent treatment with diethanolamine. Precipitation from dichloromethane by the addition of diethyl ether yielded **3d** as purple lustrous crystals with 21% yield. Mass spectrometry (ESI): $C_{22}H_{30}N_3O_2S$ requires $m/z = 400$; found $m/z = 400$.

*3.4.7. 3-N,N-Dibutylamino-7-N,N-diethanolamino-phenothiazin-5-ium iodide, **3e***

This compound was obtained following isolation of 3-*N*,*N*-dibutylamino-phenothiazin-5-ium triiodide and subsequent treatment with diethanolamine. The crude product was purified by gravity column chromatography over aluminium oxide (activated, basic, Brockmann I, std. Grade, 150 mesh, Aldrich) employing sequentially mobile phases such as ethyl acetate, 70/30 ethyl acetate/methanol and finally methanol. This gave **3e** as a purple powder (19%). Mass spectrometry (ESI): $C_{24}H_{34}N_3O_2S$ requires $m/z = 428$; found $m/z = 428$.

*3.4.8. 3-N,N-Diethanolamino-7-N,N-dipentylamino-phenothiazin-5-ium iodide, **3f***

This compound was prepared following isolation of 3-*N*,*N*-dipentylaminophenothiazin-5-ium triiodide and subsequent treatment with diethanolamine. Precipitation from dichloromethane by the addition of diethyl ether yielded **3f** as purple lustrous crystals (23%). Mass spectrometry (ESI): $C_{26}H_{38}N_3O_2S$ requires $m/z = 456$; found $m/z = 456$.

*3.4.9. 3-N,N-Dimethylamino-7-N,N-dipropylamino-phenothiazin-5-ium iodide, **3g***

This compound was prepared by isolation of 3-*N*,*N*-dipropylaminophenothiazin-5-ium triiodide and subsequent treatment with dimethylamine hydrochloride. Precipitation from dichloromethane by the addition of diethyl ether yielded **3g** as purple lustrous crystals with 20% yield. Mass spectrometry (ESI): $C_{20}H_{26}N_3S$ requires $m/z = 340$; found $m/z = 340$.

*3.4.10. 3-N,N-Diethylamino-7-N,N-dipropylaminophenothiazin-5-ium iodide, **3h***

This was prepared following isolation of 3-*N*,*N*-dipropylaminophenothiazin-5-ium triiodide and subsequent treatment with diethylamine. Precipitation from dichloromethane by the addition of diethyl ether yielded purple lustrous crystals of **3h** (15%). Mass spectrometry (ESI): $C_{22}H_{30}N_3S$ requires $m/z = 368$; found $m/z = 368$.

3.4.11. 3-N,N-Dibutylamino-7-N,N-dipropylamino-phenothiazin-5-ium iodide, **3i**

This was prepared following isolation of 3-*N*,*N*-dipropylaminophenothiazin-5-ium triiodide and subsequent treatment with dibutylamine. Precipitation from dichloromethane by the addition of diethyl ether yielded **3i** as purple lustrous crystals (19%). Mass spectrometry (ESI): $C_{26}H_{38}N_3S$ requires $m/z = 424$; found $m/z = 424$.

3.4.12. 3-N,N-Dipentylamino-7-N,N-dipropylamino-phenothiazin-5-ium iodide, **3j**

This compound was obtained following isolation of 3-*N*,*N*-dipropylaminophenothiazin-5-ium triiodide and subsequent treatment with dipentylamine. Precipitation from dichloromethane by the addition of diethyl ether yielded purple lustrous crystals of **3j** (20%). Mass spectrometry (ESI): $C_{28}H_{42}N_3S$ requires $m/z = 452$; found $m/z = 452$.

3.4.13. 3-N,N-Dihexylamino-7-N,N-dipropylamino-phenothiazin-5-ium iodide, **3k**

This was obtained following isolation of 3-*N*,*N*-dipropylaminophenothiazin-5-ium triiodide and subsequent treatment with dihexylamine. Precipitation from dichloromethane by the addition of diethyl ether yielded **3k** as purple lustrous crystals (22%). Mass spectrometry (ESI): $C_{30}H_{46}N_3S$ requires $m/z = 480$; found $m/z = 480$.

Acknowledgments

We thank Yorkshire Cancer Research for their invaluable financial support of this work, and the EPSRC Mass Spectrometry Service, Swansea, for carrying out mass spectrometry analyses.

References

[1] Brown SB, Brown EA, Walker I. The present and future role of photodynamic therapy in cancer treatment. Lancet Oncol 2004;5:497–508.
[2] Keefe KA, Tadir Y, Tromberg B. Photodynamic therapy of high-grade cervical intraepithelial neoplasia with 5-aminolevulinic acid. Lasers Surg Med 2002;31:289–93.
[3] Hillemanns P, Untch M, Dannecker C. Photodynamic therapy of vulvar intraepithelial neoplasia using 5-aminolevulinic acid. Int J Cancer 2000;85:649–53.
[4] Overholt BF, Lightdale CJ, Wang K. International multicenter partially blinded randomised study of the efficacy of photodynamic therapy using Porfimer sodium for the ablation of high-grade dysplasia in Barrett's oesophagus: results of 24 month follow-up. Gastroenterology 2003;124(Suppl.):151.
[5] Ackroyd R, Brown NJ, Davis MF. Aminolevulinic acid-induced photodynamic therapy: safe and effective ablation of dysplasia in Barrett's oesophagus. Dis Esophagus 2000;13:18–22.
[6] Lou PJ, Jones L, Hopper C. Clinical outcomes of photodynamic therapy for head and neck cancer. Technol Cancer Res Treat 2003;2:311–7.
[7] Tomaselli F, Maier A, Sankin O. Acute effects of combined photodynamic therapy and hyperbaric oxygenation in lung cancer – a clinical pilot study. Lasers Surg Med 2001;28:399–403.
[8] Copper MP, Tan IB, Oppelaar H. Meta-tetra(hydroxyphenyl)-chlorin photodynamic therapy in early-stage squamous cell carcinoma of the head and neck. Arch Otolaryngol Head Neck Surg 2003;129:709–11.
[9] Canter RJ, Mick R, Kesmodel SB. Intraperitoneal photodynamic therapy causes a capillary-leak syndrome. Ann Surg Oncol 2003;10:514–24.
[10] Nathan TR, Whitelaw DE, Chang SC. Photodynamic therapy for prostate cancer recurrence after radiotherapy: a phase I study. J Urol 2002;168:1427–32.
[11] Berr F, Wiedmann M, Tannapfel A. Photodynamic therapy for advanced bile duct cancer: evidence for improved palliation and extended survival. Hepatology 2000;31:291–8.
[12] Schick E, Ruck A, Boehnke WH, Kaufmann R. Topical photodynamic therapy using methylene blue and 5-aminolaevulinic acid in psoriasis. J Dermatol Treat 1997;8:17–9.
[13] Messmer KJ, Abel SR. Vertoporfin for age-related macular degeneration. Ann Pharmacother 2001;35:1593–8.
[14] Malik Z, Ladan H, Nitzan Y. Photodynamic inactivation of Gram-negative bacteria: problems and possible solutions. J Photochem Photobiol B 1992;14:262–6.
[15] Wainwright M. Photodynamic antimicrobial chemotherapy (PACT). J Antimicrob Chemother 1998;42:13–28.
[16] Tanielian C, Golder L, Wolf C. Production and quenching of singlet oxygen by the sensitizer in dye-sensitised photo-oxygenations. J Photochem 1984;25:117–25.
[17] Tanielian C, Wolff C, Esch M. Singlet oxygen production in water: aggregation and charge-transfer effects. J Phys Chem 1996;100:6555–60.
[18] Creagh TA, Gleeson M, Travis D, Grainger R, McDermott TED, Butler MR. Is there a role for in vivo methylene blue staining in the prediction of bladder tumour recurrence. Br J Urol 1995;75:477–9.
[19] Jacobi A. J Am Med Assoc 1906;47:1545–6.
[20] Williams JL, Stamp J, Devonshire R, Fowler GJS. Methylene blue and the photodynamic therapy of superficial bladder cancer. J Photochem Photobiol B 1989;4:229–34.
[21] Fowler GJS, Rees RC, Devonshire R. The photokilling of bladder carcinoma cells in vitro by phenothiazine dyes. Photochem and Photobiol 1990;52(3):489–94.
[22] Wainwright M, Phoenix DA, Marland L, Wareing DRA, Bolton FJ. A study of photobactericidal activity in the phenothiazinium series. FEMS Immunol Med Microbiol 1997;19:75–80.
[23] Wainwright M, Phoenix DA, Laycock SL, Wareing DRA, Wright PA. Photobactericidal activity of phenothiazinium dyes against methicillin-resistant strains of *Staphylococcus aureus*. FEMS Microbiol Lett 1998;160:177–81.
[24] Lambrecht B, Norley SG, Kurth R, Mohr H. Rapid inactivation of HIV-1 in single donor preparations of human fresh frozen plasma by Methylene blue/light treatment. Biologicals 1994;22:227–31.
[25] Skripchenko A, Robinette D, Wagner SJ. Comparison on Methylene blue and Methylene violet for photoinactivation of intracellular and extracellular virus in red cell suspensions. Photochem Photobiol 1997;65(3):451–5.
[26] Bellin JS, Mohos SC, Oster G. Dye sensitised photoinactivation of tumour cells in vitro. Cancer Res 1961;21:1365–71.
[27] Rice L, Wainwright M, Phoenix D. Phenothiazine photosensitisers. III. Activity of Methylene Blue derivatives against pigmented melanoma cell lines. J Chemother 2000;12:94–104.
[28] Frimberger AE, Moore AS, Cincotta L, Cotter SM, Foley JW. Photodynamic therapy of naturally occurring tumours in animals

using a novel benzophenothiazine photosensitiser. Clin Cancer Res 1998;4:2207–18.
[29] Ball DJ, Luo Y, Kessel D, Griffiths J, Brown SB, Vernon DI. The induction of apoptosis by a positively charged Methylene blue derivative. J Photochem Photobiol B 1998;42:159–63.
[30] Tremblay JF, Dussault S, Viau G, Gad F, Boushira M, Bissonnette R. Photodynamic therapy with Toluidine blue in Jurkat cells: cytotoxicity, subcellular localisation and apoptosis induction. Photochem Photobiol Sci 2002;1:852–6.
[31] Cincotta AH, Cincotta L, Foley JW. Novel benzophenothiazinium photosensitisers: preliminary in-vivo results. In: SPIE Proc vol. 1203. 1990. p. 202–10.
[32] Cincotta AH, Foley JW. US 4962197.
[33] Wagner SJ, Skripchenko A, Robinette D, Foley JW, Cincotta L. Factors affecting virus photoinactivation by a series of phenothiazine dyes. Photochem Photobiol 1998;67(3):343–9.
[34] Wainwright M, Phoenix DA, Rice L, Burrow SM, Waring JJ. Increased cytotoxicity and phototoxicity in the methylene blue series via chromophore methylation. J Photochem Photobiol B 1997;40:233–9.
[35] Mellish KJ, Cox RD, Vernon DI, Griffiths J, Brown SB. In vitro photodynamic activity of a series of Methylene blue analogues. Photochem Photobiol 2002;75(4):392–7.
[36] Walker I, Gorman SA, Cox RD, Vernon DI, Griffiths J, Brown SB. A comparative analysis of phenothiazinium salts for the photosensitisation of murine fibrosarcoma (RIF-1) cells in vitro. Photochem Photobiol Sci 2004;3:653–9.
[37] Strekowski L, Hou D-F, Wydra R. A synthetic route to 3-(dialkylamino)phenothiazin-5-ium salts and 3,7-disubstituted derivatives containing two different amino groups. J Heterocyclic Chem 1993;30:1693–5.
[38] Moor AC. Signalling pathways in cell death and survival after photodynamic therapy. J Photochem Photobiol B 2000;57:1–13.
[39] Bell AL. The development of methods for assessing the properties of new photosensitisers for use in photodynamic therapy. PhD thesis, University of Leeds; 2002.